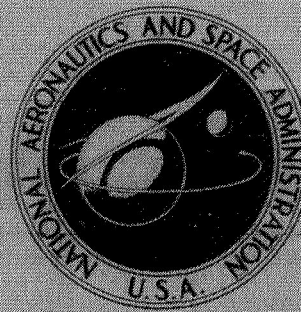


CASE FILE
COPY

N70-38549

NASA TECHNICAL
MEMORANDUM



NASA TM X-2093

NASA TM X-2093

ANALYSIS OF LAUNCH WINDOWS
FROM ELLIPTICAL ORBITS FOR
REPRESENTATIVE MARS MISSIONS

by Larry A. Manning and Byron L. Swenson

Office of Advanced Research and Technology

Mission Analysis Division

Moffett Field, Calif. 94035

NATIONAL AERONAUTICS AND SPACE ADMINISTRATION • WASHINGTON, D. C. • SEPTEMBER 1970

1. Report No. NASA TM X-2093		2. Government Accession No.		3. Recipient's Catalog No.	
4. Title and Subtitle ANALYSIS OF LAUNCH WINDOWS FROM ELLIPTICAL ORBITS FOR REPRESENTATIVE MARS MISSIONS				5. Report Date September 1970	
				6. Performing Organization Code	
7. Author(s) Larry A. Manning and Byron L. Swenson				8. Performing Organization Report No. A-3638	
9. Performing Organization Name and Address Office of Advanced Research and Technology Mission Analysis Division Moffett Field, California 94035				10. Work Unit No. 130-06-05-02-15	
				11. Contract or Grant No.	
12. Sponsoring Agency Name and Address National Aeronautics and Space Administration Washington, D.C. 20546				13. Type of Report and Period Covered Technical Memorandum	
				14. Sponsoring Agency Code	
15. Supplementary Notes					
16. Abstract <p>Round trips to Mars have been investigated to define representative launch windows (i.e., allowable staytime variations) for Mars departures from elliptical orbits and the associated propulsive velocity requirements. The 1982 inbound and 1986 outbound Venus swingby opportunities were selected for analysis and serve to demonstrate the influence of the interplanetary trajectory characteristics on the launch window propulsive velocity requirements. These velocity requirements are the sum of the Mars arrival and departure maneuvers. This report presents contour maps indicating the effects on the launch window of velocity capability (total ΔV), transfer technique, orbit inclination, and orbit eccentricity. Use of one-, two-, and three-impulse transfers from the Mars orbit to the Earth return trajectory were investigated. For all cases, insertion at planet arrival was into an orbit coplanar with the arrival asymptote and any required plane change was performed during the planet departure phase.</p> <p>Two specific conclusions can be drawn from the results of this study. First, as a result of the effectiveness of the three-impulse transfer in reducing the ΔV requirement to a nearly constant value regardless of the orbit geometry, the orbit selection can be optimized from other considerations (i.e., science, communication, power, etc.) independent of the interplanetary trajectory considerations. Second, for highly elliptical orbits ($e = 0.7$) a total ΔV (arrival plus departure) at Mars that is 1 km/sec below the minimum coplanar requirement for circular parking orbits provides staytimes of 60 days and usually allows any orbit inclination to be used. This ΔV is effectively 2 km/sec below that required for circular orbits with the same allowable staytime. In addition, whereas the circular orbits require three impulses at departure, for some missions a single impulse can be used to eject from the elliptical orbit.</p>					
17. Key Words (Suggested by Author(s)) Elliptical orbits Multi-impulse transfers Mars staytime Round trips			18. Distribution Statement Unclassified - Unlimited		
19. Security Classif. (of this report) Unclassified		20. Security Classif. (of this page) Unclassified		21. No. of Pages 29	
				22. Price* \$3.00	

TABLE OF CONTENTS

	Page
NOTATION	v
SUMMARY	1
INTRODUCTION	1
METHOD OF ANALYSIS	2
Orbit Geometry	2
Transfer Techniques	4
Nominal Missions	4
Impulsive Maneuvers	6
NUMERICAL ANALYSIS	7
Launch Window Development	7
Launch Window Comparison	12
CONCLUDING REMARKS	14
APPENDIX A – SINGLE IMPULSE ANALYSIS	15
APPENDIX B – TWO IMPULSE ANALYSIS	20
REFERENCES	23

NOTATION

a	semimajor axis, km
e	eccentricity
H	altitude, km
I_{∞}	minimum angle between departure vector and orbit plane, deg
i	inclination, deg
J_2	second harmonic of planetary oblateness
R	planet radius, km
t	time, sec
ΔV	propulsive velocity increment, km/sec
V_{∞}	hyperbolic excess velocity, km/sec
x,y,z	components of the planet centered coordinate system
δ	declination, deg
τ	unperturbed orbital period, sec
ρ	right ascension, deg
Ω	longitude of ascending node, deg
ω	argument of periapsis, deg

Subscripts

h	hyperbola
i	intermediate or departure ellipse
o	original parking orbit ellipse
p	periapsis

ANALYSIS OF LAUNCH WINDOWS FROM ELLIPTICAL ORBITS FOR REPRESENTATIVE MARS MISSIONS¹

Larry A. Manning and Byron L. Swenson

Office of Advanced Research and Technology
Mission Analysis Division
Moffett Field, California 94035

SUMMARY

Round trips to Mars have been investigated to define representative launch windows (i.e., allowable staytime variations) for Mars departures from elliptical orbits and the associated propulsive velocity requirements. The 1982 inbound and 1986 outbound Venus swingby opportunities were selected for analysis and serve to demonstrate the influence of the interplanetary trajectory characteristics on the launch window propulsive velocity requirements. These velocity requirements are the sum of the Mars arrival and departure maneuvers. This report presents contour maps indicating the effects on the launch window of velocity capability (total ΔV), transfer technique, orbit inclination, and orbit eccentricity. Use of one-, two-, and three-impulse transfers from the Mars orbit to the Earth return trajectory were investigated. For all cases, insertion at planet arrival was into an orbit coplanar with the arrival asymptote and any required plane change was performed during the planet departure phase.

Two specific conclusions can be drawn from the results of this study. First, as a result of the effectiveness of the three-impulse transfer in reducing the ΔV requirement to a nearly constant value regardless of the orbit geometry, the orbit selection can be optimized from other considerations (i.e., science, communication, power, etc.) independent of the interplanetary trajectory considerations. Second, for highly elliptical orbits ($e = 0.7$) a total ΔV (arrival plus departure) at Mars that is 1 km/sec below the minimum coplanar requirement for circular parking orbits provides staytimes of 60 days and usually allows any orbit inclination to be used. This ΔV is effectively 2 km/sec below that required for circular orbits with the same allowable staytime. In addition, whereas the circular orbits require three impulses at departure, for some missions a single impulse can be used to eject from the elliptical orbit.

INTRODUCTION

Elliptical parking orbits are receiving increased attention for use as planetary parking orbits during interplanetary exploration. These orbits have been shown to greatly reduce the propulsive requirements for arrival and departure at the target planet (ref. 1). In addition, orbital plane

¹The material in this report was summarized in a paper by the same authors and Jerry M. Deerwester, and entitled "Launch Window Analysis for Round Trip Mars Missions," presented at the Canaveral Council of Technical Societies' Fifth Space Congress, Cocoa Beach, Florida, March 11-14, 1968.

changes can be performed with a lower propulsion system requirement for elliptical orbits than for the low circular orbits generally considered for planetary exploration.

Selection of the orbit inclination at the planet is made after consideration of the mission science requirements (optical coverage, probes, landers, etc.) and of the effect of that inclination on the mission propulsive requirements. This second effect is particularly significant since the orbit plane will not, in general, contain both the arrival and the departure velocity vectors. Thus it is necessary to perform a plane change maneuver, which can be costly in terms of propulsive requirements.

This report presents the results of an analysis of the influence of elliptic orbit inclinations on the staytime in orbit and the associated energy requirements for representative round trip Mars missions in a similar manner previously used for circular orbits (ref. 2). In addition to the orbit itself, the technique used to transfer between the orbit and the interplanetary trajectory is analyzed. Three techniques are considered. They are: (1) single impulse; (2) two impulse, the first of which provides all the plane change and the second all the velocity change, and (3) three impulse, which uses an intermediate ellipse of high eccentricity from which all the plane change is made.

To ensure realistic results, specific missions were selected for the analysis. The strong coupling of the orbit and both legs of the interplanetary transfer is such that an analysis of the orbit transfer technique by itself, while interesting, does not provide the insight necessary to allow proper mission/spacecraft tradeoffs. Two missions, encompassing the four trajectory types of primary interest (i.e., direct outbound and inbound, and Venus swingby outbound and inbound), were chosen as representative of future round trips of interest. While the numerical results obtained are not directly applicable to other Mars missions, the data trends and resulting conclusions are generally applicable.

The report is divided into two major sections. The first describes the basic parts of the study, that is, the orbit geometry, the orbit transfer techniques, and the nominal missions descriptions. The second couples the representative missions with the orbit characteristics to provide contour maps of constant velocity increments as functions of inclination and staytime in orbit.

METHOD OF ANALYSIS

Orbit Geometry

In considering the launch window problem for a given mission, it is first necessary to establish the relative positions of the orbit plane and the hyperbolic escape asymptote with time. For the analysis of planetary launch windows, it was assumed that the parking orbit at planet arrival was coplanar with the arrival asymptote and was established by a tangential impulse not necessarily at periapsis. The resulting orbit elements are shown in figure 1. As indicated, a planet-centered right-hand coordinate system with Z axis at the north pole and X axis at the planet vernal equinox was chosen. The arrival asymptote or hyperbolic excess velocity vector is defined conventionally as a planet centered vector with right ascension ρ and declination δ . The orbit elements of interest, that is, the inclination i and longitude of the ascending node Ω are related by

$$\sin(\rho - \Omega) = \frac{\tan \delta}{\tan i}$$

for all $i > \delta$, while the argument of periapsis ω is measured in the orbit plane from the ascending node.

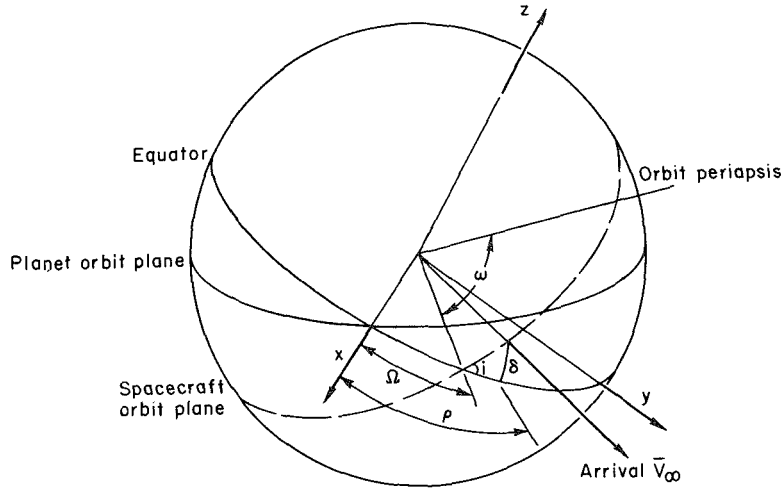


Figure 1.- Orbit geometry at planet arrival.

It can be seen that for each inclination there are two orbit planes coplanar with the arrival asymptote. These two orbits can be distinguished by the relative positions of the spacecraft approach vector at the time of the final midcourse maneuver and the planet centered excess velocity vector. If the spacecraft approaches above the excess velocity vector, it moves initially toward the north pole of the planet and the magnitude of $(\rho - \Omega)$ will be greater than 90° . This orientation will be referred to as a northern insertion. In the other case, the spacecraft approaches below the excess velocity vector (i.e., toward the south pole) and the magnitude of $(\rho - \Omega)$ is less than 90° . Figure 1 illustrates this configuration, which is called a southern insertion.

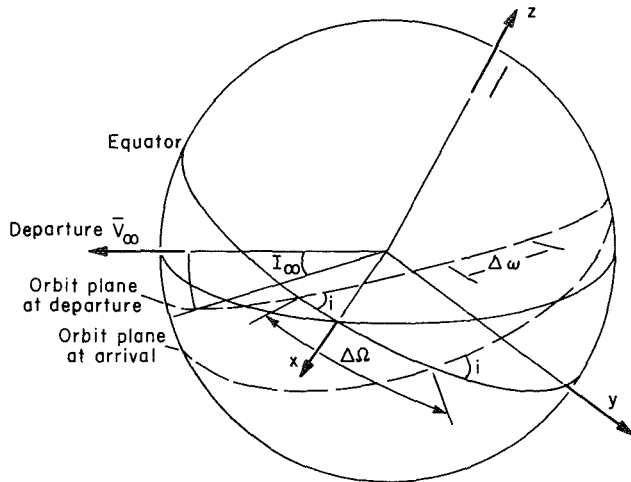


Figure 2.- Orbit geometry at planet departure.

The situation at some time after arrival is illustrated in figure 2. The perturbation due to planet oblateness causes the orbit plane to regress about the planet in the manner shown. That is, the inclination of the orbit remains unchanged, the longitude of the ascending node changes by $\Delta\Omega$, and the argument of periapsis changes by $\Delta\omega$ where, to first order in the planet oblateness (ref. 3)

$$\Delta\Omega = 3\pi J_2 \left(\frac{R}{p} \right)^2 (\cos i) N$$

$$\Delta\omega = 3\pi J_2 \left(\frac{R}{p} \right)^2 \left(2 - \frac{5}{2} \sin^2 i \right) N$$

with the number of perturbed orbits (N) and the semilatus rectum (p) defined by

$$N = \frac{t}{\tau} \left[1 + \frac{3}{2} J_2 \left(\frac{R}{p} \right)^2 \left(1 - \frac{3}{2} \sin^2 i \right) (1 - e^2)^{1/2} \right]$$

$$p = a(1 - e^2)$$

At that time, the orbit plane makes an angle I_∞ with the departure asymptote. This is the angle that must be compensated for during the departure maneuver.

Transfer Techniques

Three transfer techniques were considered for the departure maneuver: an optimum single impulse, a constrained two impulse, and a three-impulse transfer.

One-impulse technique— In this technique, since at a given time both the departure hyperbolic excess vector and the characteristics of the parking orbit at departure are fixed, the optimum noncoplanar, nontangential departure maneuver true anomaly is established by a numerical method. In general, the minimum total ΔV for arrival plus departure requires an off-periapsis arrival and both an off-periapsis and a nonminimum plane change angle maneuver at departure. The associated equations are described in appendix A.

Two-impulse technique— The first impulse is applied at apoapsis to perform the required plane change. The second impulse is applied tangentially near periapsis and provides the required velocity change to achieve the desired excess velocity. The associated equations are described in appendix B.

Three-impulse technique— The first impulse is applied at periapsis to increase the orbit eccentricity; a value of 0.9 was used for the eccentricity of the intermediate ellipse. The second impulse performs the necessary plane-change maneuver at apoapsis, and the third impulse applied near periapsis provides the additional velocity increment necessary to achieve the desired hyperbolic trajectory. The second and third impulses of this technique are computationally the same as those in appendix B for the two-impulse transfer. The first impulse serves to raise the apoapsis altitude, thus reducing the subsequent plane change velocity increment for a given I_∞ . This sequence is an approximation of the optimal velocity/plane change distribution between the three maneuvers (ref. 4).

Nominal Missions

To obtain meaningful operation data and conclusions on launch windows, it is necessary to define reasonably representative round trip missions. The missions selected as representative of those most likely to be used are the 1982 inbound Venus swingby and the 1986 outbound Venus swingby. The study assumed a single outbound (Earth to Mars) leg for each mission independent of the staytime. The inbound (Mars to Earth) leg was defined as a function of staytime for each opportunity considered, to establish the Mars departure velocity vector variation. The mission selection procedures and criteria are discussed fully in a previous report on circular orbits (ref. 2).

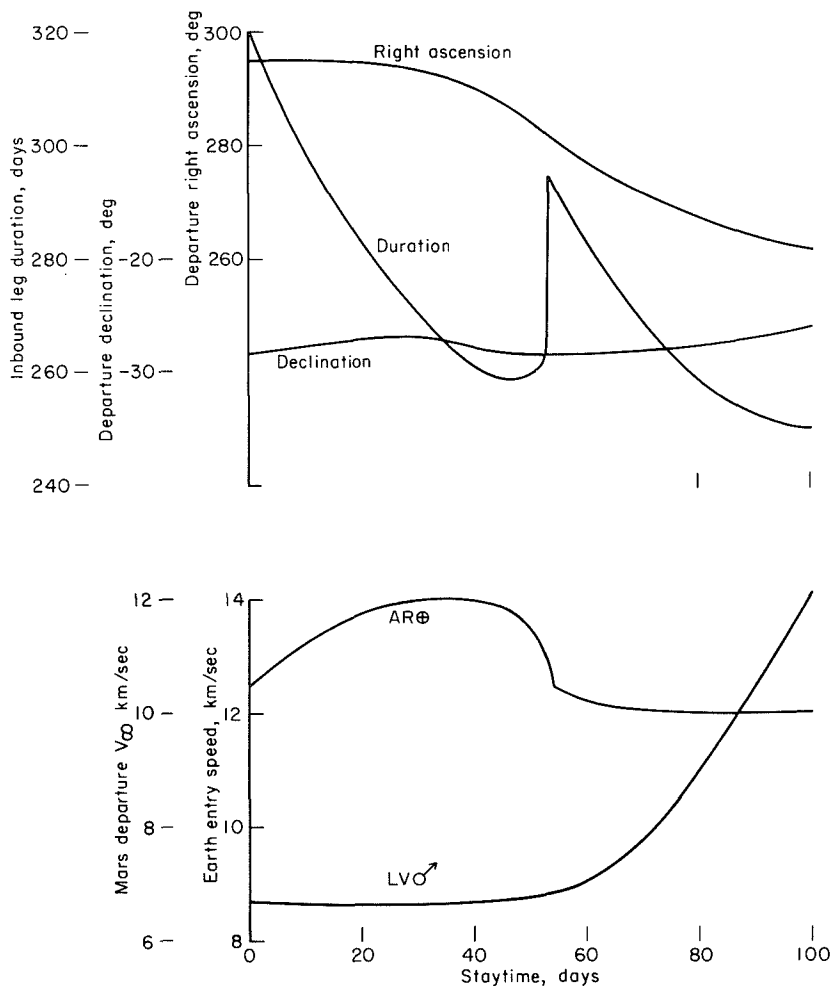
The outbound leg characteristics are delineated in table 1, while the characteristics of the inbound legs are shown as a function of staytime in figures 3(a) and (b). The break in the curves of figure 3(b) occurs where the central angle of the 1986 inbound leg is nearly equal to 180° .

TABLE 1.- NOMINAL OUTBOUND LEG CHARACTERISTICS

Opportunity year	Leave Earth					Pass Venus		Arrive Mars			
	Date ^a	V_∞ , km/sec	ΔV , ^b km/sec	ρ , deg	δ , deg	Date ^a	r_p/R_\oplus	Date ^a	V_∞	ρ	δ
1982	4990	4.6	4.3	145.4	-0.6	---	---	5210	3.7	288.1	-4.4
1986	6160	4.6	4.3	74.5	19.9	6317	1.76	6500	6.0	285.0	-20.8

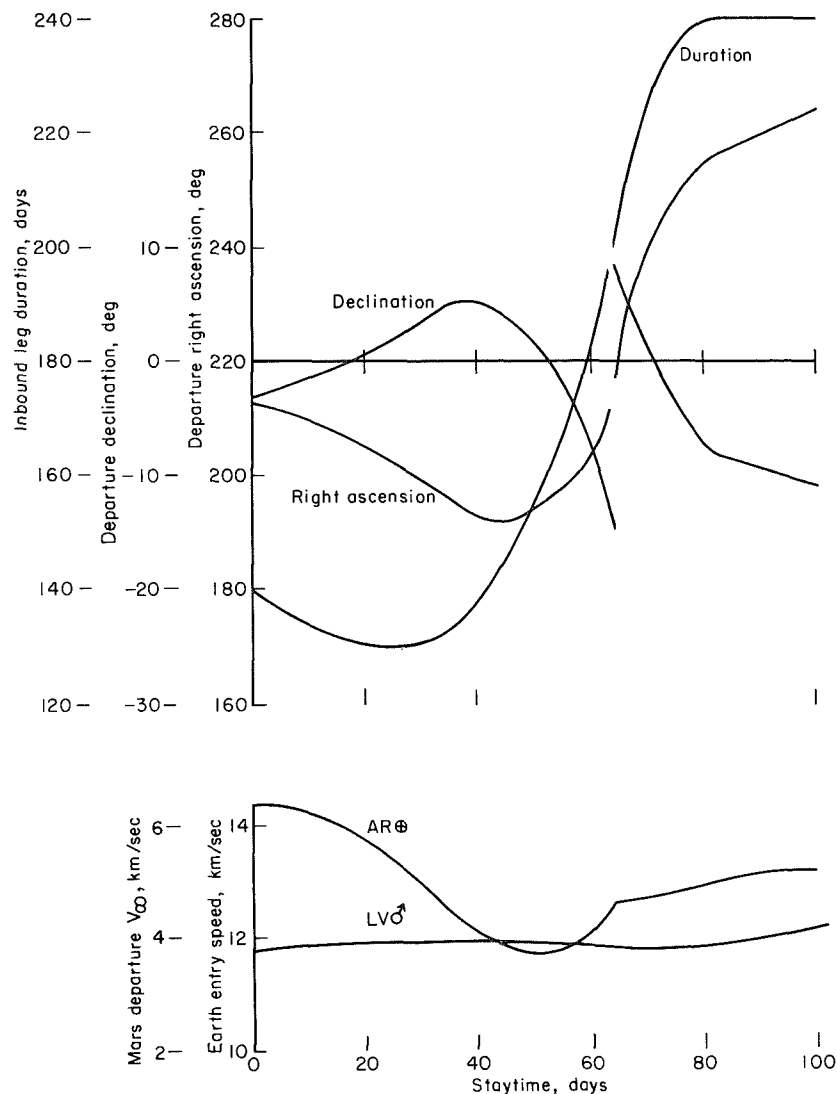
^aAll dates are Julian minus 244 0000

^b150-km circular orbit



(a) 1982 inbound swingby (Mars arrival date = 244 5210).

Figure 3.- Inbound leg trajectory characteristics.



(b) 1986 outbound swingby (Mars arrival date = 244 6500).

Figure 3.- Concluded.

Impulsive Maneuvers

This analysis assumes that the velocity increments are applied impulsively, and one effect of this assumption is the neglect of gravity losses. Gravity losses, however, are small (i.e., 5 percent of the total velocity requirement for an I_{sp} of 1000 sec (ref. 5) decreasing to about 3 percent for a chemical system I_{sp} of 400 sec (ref. 6)) and can be neglected without significant error. It has also been shown that the orientation between the parking orbit and the escape hyperbola is preserved whether the velocity addition is impulsive or through a finite thrusting time, although the true anomaly of ignition point varies slightly between the two assumptions (ref. 2).

NUMERICAL ANALYSIS

Launch Window Development

In this study, the sum of the arrival and the departure ΔV requirements was used as a measure of the relative performance of the three transfer techniques and to define the staytime variation (launch window) for a given energy level. This summation approach is necessary since the location of the elliptical orbit periapsis relative to the arrival or departure velocity vector exercises a major influence on the magnitude of the transfer ΔV .

A single-impulse coplanar insertion maneuver was assumed at arrival. If this maneuver is a tangential, periapsis insertion (i.e., minimum arrival ΔV), the departure maneuver, after a given staytime, may require an excessively large ΔV to compensate for its being performed significantly off the optimum departure location. An off-pericenter insertion maneuver at arrival can reduce the off-pericenter requirement at departure and thereby lower the sum of the ΔV . This is a reflection of the fact that coplanar maneuvers as much as 30° to 40° off-periapsis can be made for a ΔV penalty of about 2 percent or less (ref. 2). The value of the optimal off-pericenter angle at arrival is a function of the inclination of the parking orbit and the desired staytime at the planet.

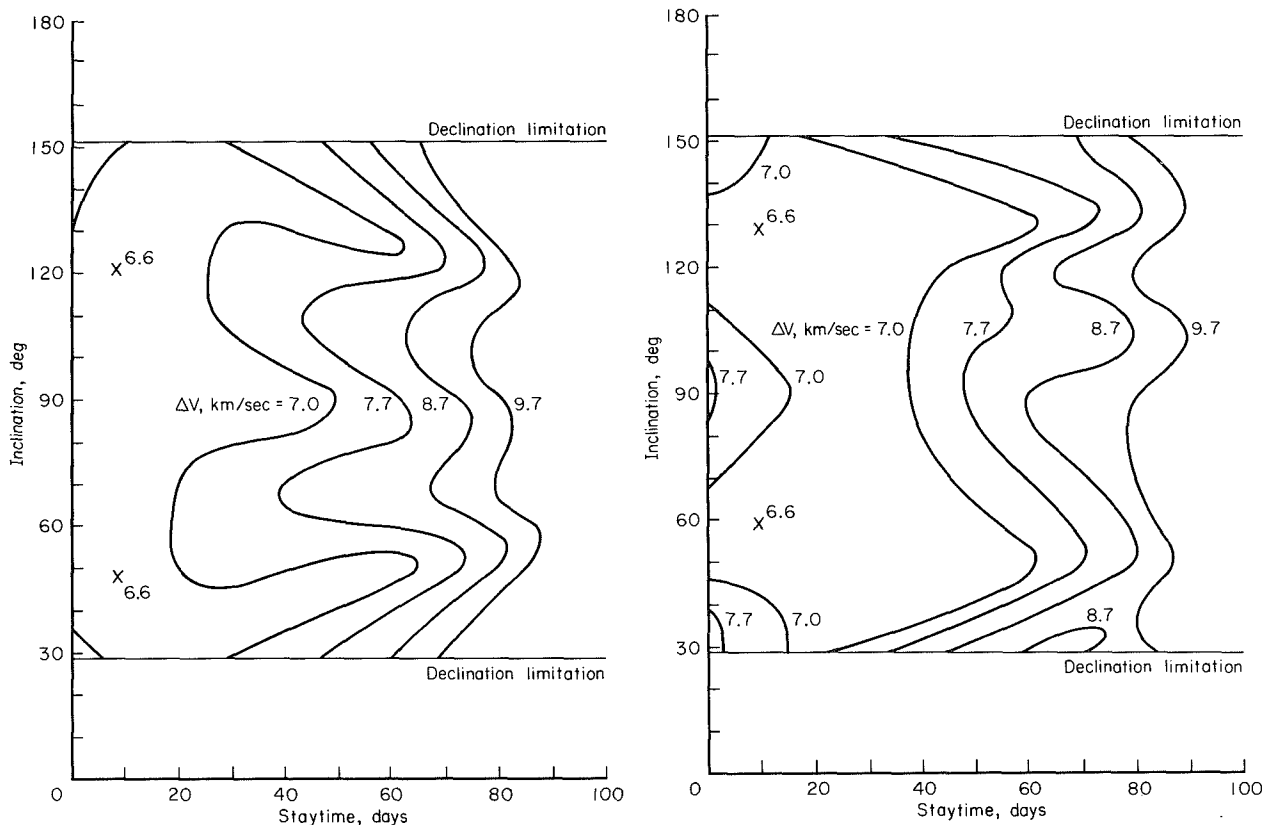
To assess the launch window requirements, a nominal staytime (30 days) is selected, and the optimum insertion and departure maneuvers (found by varying the orbit-insertion point for $+90^\circ$ to -90° true anomaly on the parking orbit) for that staytime are defined for each inclination. The insertion maneuver is then held fixed for each inclination, and the staytime is varied to determine the total ΔV requirement. From these results, the available departure launch window for a given ΔV capability is determined. Reselection of the insertion maneuver would be expected to produce some gains, but based on the few cases investigated, changes that resulted in reduced ΔV at longer than nominal staytimes also resulted in increased ΔV for shorter than nominal staytimes. Such a tradeoff would be of interest during a study of a particular mission but adds little to the general discussion presented here.

The minimum inclination that will allow coplanar arrival and departure is defined by the magnitude of the larger of the declinations at arrival and departure. This inclination is 28.7° and 20.8° for the 1982 and 1986 missions, respectively. The maximum inclination that will allow coplanar arrival and departure is 180° minus the minimum inclination (i.e., a retrograde orbit). Therefore to obtain the parametric information contained in this report, the orbit inclination was varied from 30° to 150° for both missions in 10° intervals. Parking orbit eccentricities of 0.3, 0.5, and 0.7 were assumed with a periapsis altitude of 300 km. Both northern and southern insertion directions were considered.

To decrease the volume of data but still outline the salient features of elliptical parking orbits, data are presented only for the better insertion direction of each year (i.e., northern insertion for 1982 and southern insertion for 1986). In addition, neither data for an orbit eccentricity of 0.5 nor data for two-impulse transfers are presented since they resulted in no increased understanding of the problem and were generally bounded by the data shown.

1982 inbound swingby— Figure 4(a) presents the total ΔV contours (arrival plus departure) for a one-impulse transfer from an elliptical orbit of 0.3 eccentricity as a function of inclination and staytime. If a coplanar periapsis arrival and departure were possible, a minimum ΔV of 6.6 km/sec could be achieved. As can be seen in figure 4(a), two small regions exist for which the arrival and departure conditions are sufficiently near the absolute optimum that essentially no penalty occurs. A 6-percent increase (0.4 km/sec) in the total ΔV results in a staytime of at least 20 days for all inclinations, and as much as 50 days for a polar orbit. Using the total ΔV representative of minimum launch windows for circular orbits (7.7 km/sec), a staytime of at least 40 days exists for all inclinations, compared with the 5-day staytime for the one-impulse transfer from circular orbits (ref. 2).

Data for a three-impulse transfer from a 0.3 eccentricity orbit are shown in figure 4(b). Note that some increase in launch window duration for a given velocity capability occurs over that for a one-impulse transfer. However, the increase is not large due to the close positions of the arrival vector and the departure vector and their relative magnitudes. For this year, the arrival and departure pericenters are located so that both maneuvers can be performed with one impulse near the orbit pericenter because of the small plane-change requirement. A ΔV of 7.7 km/sec would produce a launch window of about 48 days for any inclination except those that are near equatorial.



(a) 1982 inbound swingby; northern insertion; parking orbit eccentricity = 0.3; one impulse.

(b) 1982 inbound swingby; northern insertion; parking orbit eccentricity = 0.3; three impulse.

Figure 4.- Mars ΔV contours.

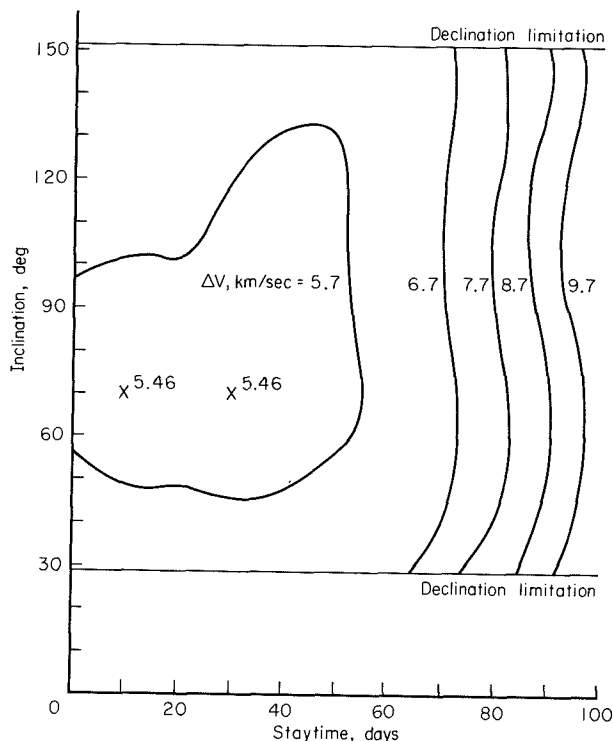


Figure 5.- Mars ΔV contours; 1982 inbound insertion; northern insertion; parking orbit eccentricity = 0.7; one impulse.

Figure 5 presents the contour plot for a one-impulse transfer from a 0.7 eccentricity parking orbit. For this orbit, the minimum possible ΔV requirement is 5.45 km/sec, which is nearly achieved in two regions of figure 5. An increase of 5 percent in ΔV to 5.7 km/sec allows a window of 50 days for near polar and high-inclination posigrade orbits. The particular form of this ΔV contour in the retrograde region is of interest in that it indicates a maximum staytime of up to 50 days for a ΔV of 5.7 km/sec, but also a minimum staytime of 20 to 40 days for the same velocity capability. If this early departure restriction is of concern, then the ΔV requirements for retrograde orbits are higher than those for posigrade orbits for the same launch window. Use of a ΔV of 7.7 km/sec results in a launch window of 75 days for nearly all inclinations.

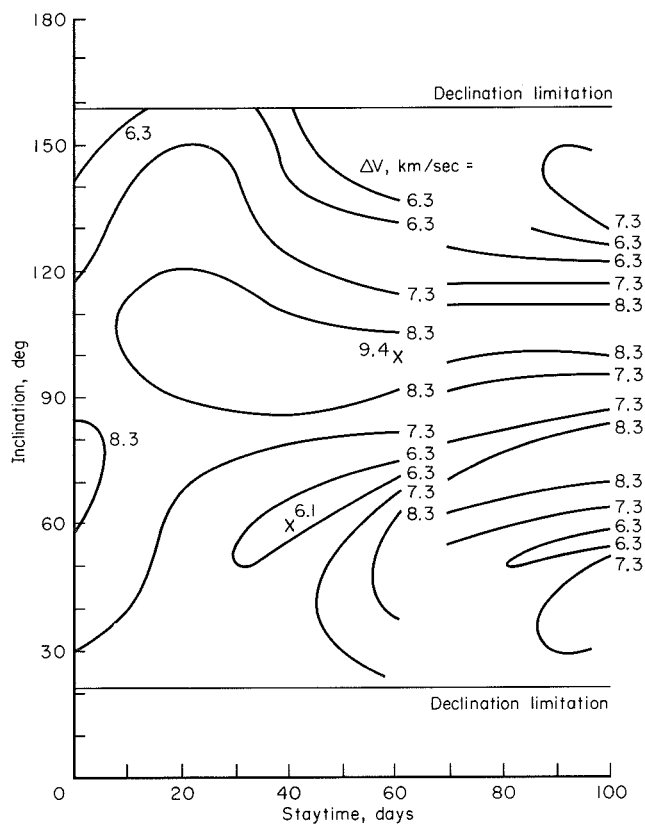
The use of a three-impulse transfer from this orbit eccentricity does not significantly change the launch window contour, for reasons given above; therefore it is not shown.

1986 outbound swingby— Data for a one-impulse transfer from a 0.3 eccentricity parking orbit is shown in figure 6(a). A minimum ΔV requirement of 6.0 km/sec exists for the idealized coplanar, pericenter maneuvers; a minimum of 6.1 km/sec was actually achieved. Since the arrival and the departure asymptotes differ over 45° in right ascension, a ΔV of 8.3 km/sec must be allowed before a generally available launch window exists for most inclinations at all staytimes. As a result, the one-impulse case requires a serious compromising of the departure maneuver. The difference in right ascension also results in the contour figure becoming nonsymmetric about the polar orbit. This nonsymmetry is such that retrograde orbits provide the maximum launch window for a given ΔV capability as can be seen in all the curves for the 1986 mission.

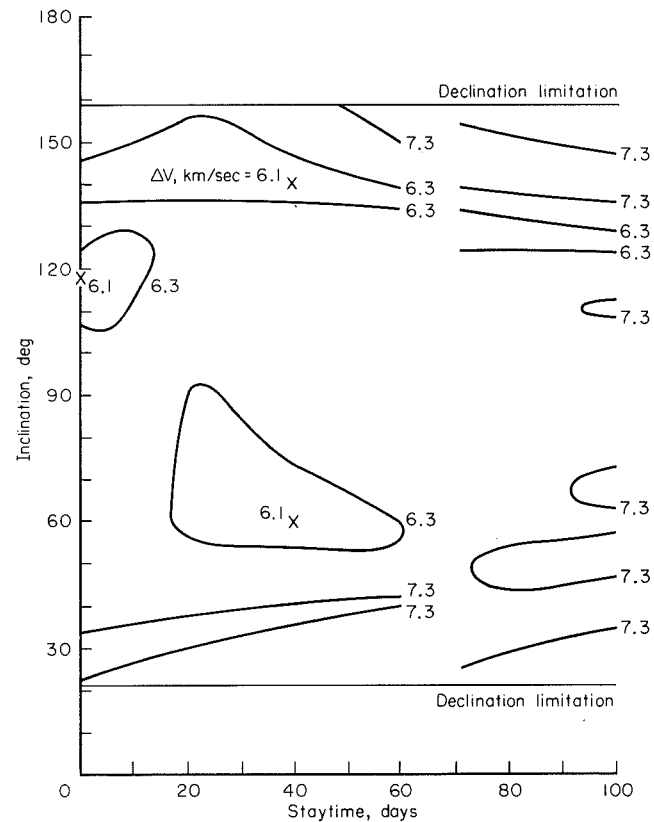
Figure 6(b) presents the contour maps for the three-impulse transfer. In this case, as compared to 1982, the large plane-change requirement allows for effective use of the three-impulse technique and thus results in a significant increase in the available launch window. The use of a total ΔV representative of minimum launch windows for circular orbits (7.3 km/sec) results in a launch window of over 60 days for almost all inclinations.

The contour map for a one-impulse transfer from a 0.7 eccentricity orbit is shown in figure 7(a). For this orbit, the minimum ΔV requirement would be 4.85 km/sec. Such a low value was not achieved anywhere on the one-impulse transfer plot. A ΔV of 7.3 km/sec opens the region below 50° and above 120° inclination for staytimes of 100 days. A ΔV of 8.0 km/sec allows use of the entire contour map.

The results of using a three-impulse transfer from the 0.7 eccentricity orbit are shown in figure 7(b). Here a ΔV of 6.3 km/sec opens essentially the entire map to use, while a ΔV of only 5.3 km/sec would allow any retrograde orbit.

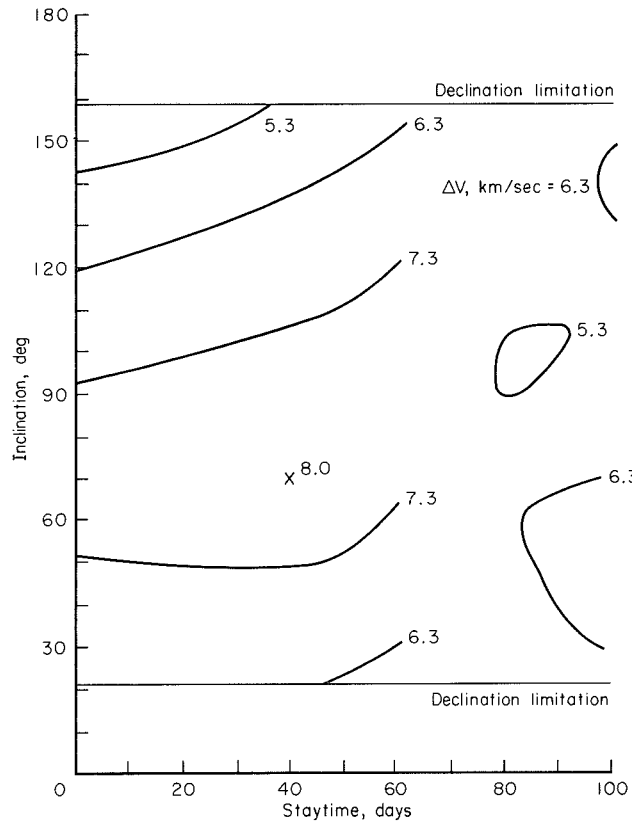


(a) 1986 outbound swingby; southern insertion; parking orbit eccentricity = 0.3; one impulse.

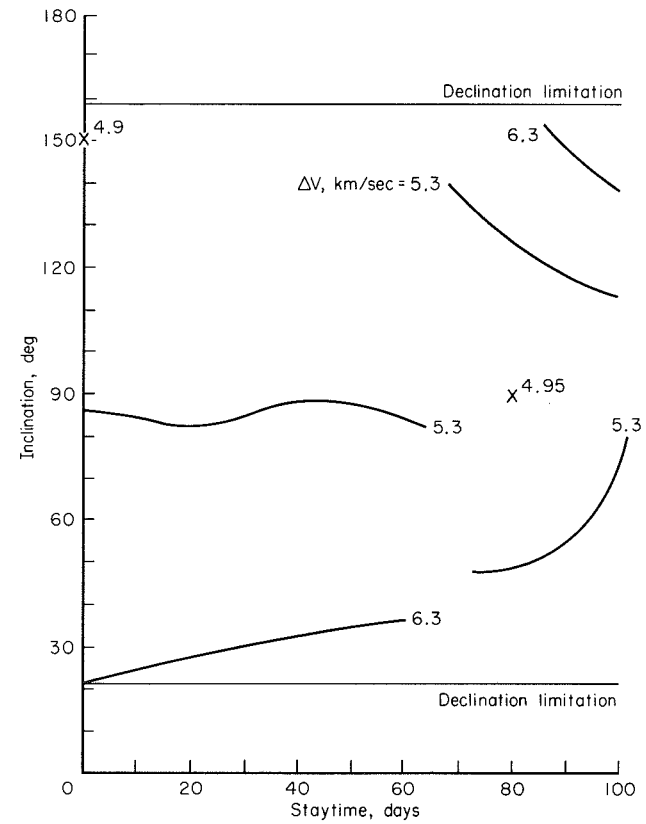


(b) 1986 outbound swingby; southern insertion; parking orbit eccentricity = 0.3; three impulse.

Figure 6.- Mars ΔV contours.



(a) 1986 outbound swingby; southern insertion; parking orbit eccentricity = 0.7; one impulse.



(b) 1986 inbound insertion; northern insertion; parking orbit eccentricity = 0.7; three impulse.

Figure 7.- Mars ΔV contours.

Launch Window Comparison

The previous sections have indicated in a parametric manner the effects of orbital parameters, transfer techniques, and interplanetary trajectories on the available launch window (i.e., allowable staytime variation) at Mars. In this section, the data are compared with those previously published for circular orbits (ref. 2) to provide insight into the potential tradeoffs among the pertinent system parameters (i.e., orbit eccentricity, energy requirements, number of impulses, trajectory, and staytime). For the comparison, a fixed total propulsive velocity requirement (arrival plus departure) of 8.7 km/sec was used for the 1982 opportunity. Figure 8 shows that for circular orbits, use of single impulse at this energy level allows staytimes of up to 35 days for all inclinations and up to 70 days for specific inclinations. Use of three impulses makes the 70-day staytime available at all inclinations. With an orbit of intermediate eccentricity ($e = 0.3$), all inclinations have allowable staytimes up to 80 days with the optimal number of impulses depending on the particular inclination. This overlap is due to the method of selecting the arrival maneuvers and the small difference between the right ascensions and declinations of the arrival and departure vectors for the 1982 mission. Use of a highly eccentric orbit ($e = 0.7$) results in essentially identical performance for the one- and three-impulse transfers. Staytimes of 90 days are readily available.

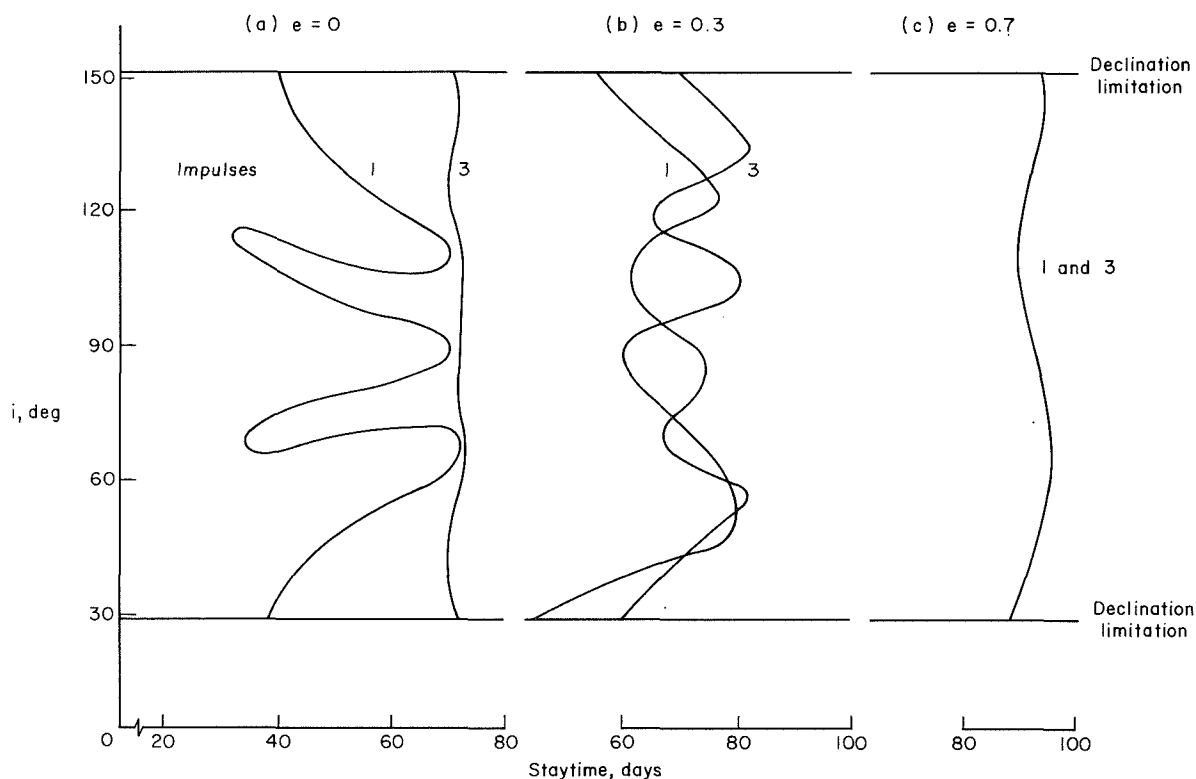


Figure 8.- Effect of eccentricity on launch window 1982 inbound swingby; total $\Delta V = 8.7$ km/sec northern insertion.

Comparison of the circular and highly elliptical orbits reveals that for specific values of inclination they have nearly the same staytimes if a single impulse is employed; however, only the highly elliptical orbit allows the use of all inclinations at this energy level for the maximum staytime. Use of three impulses allows circular orbits to provide nearly the same staytime variation as the one-impulse elliptical. The major advantage of elliptical orbits is that the

total ΔV requirement can be reduced below the circular orbit level for the same staytime. Referring back to figure 5, it can be seen that for $e = 0.7$, a ΔV of only 6.7 km/sec can produce an allowable staytime of 70 days for all inclinations.

Thus, an elliptical orbit ($e = 0.7$) with a one-impulse transfer can provide the same launch window as a circular orbit with a three-impulse departure while allowing a savings of 2 km/sec in the propulsive velocity requirement. Another advantage is the reduced complexity afforded by a single velocity maneuver at arrival and one at departure, although the effect of the elliptical orbit on operations at the planet may be undesirable.

The 1986 mission is representative of missions with significant variations between the arrival and departure vectors. For the 1986 mission, a total ΔV of 7.3 km/sec for arrival plus departure was used. Figure 9 compares the allowable staytime for circular and elliptical orbits at this energy level. The shaded areas represent those regions of orbit inclination and staytime where the sum of the arrival and departure velocity maneuvers requires a velocity capability greater than 7.3 km/sec. The contours are unsymmetrical because of the velocity vector differences discussed, and near polar orbits are not available at this energy level for the single-impulse transfers. There are staytimes exceeding 60 days, but these are not shown since the contour lines become complex when the central angle of the trajectory from Mars to Earth exceeds 180° (e.g., fig. 6).

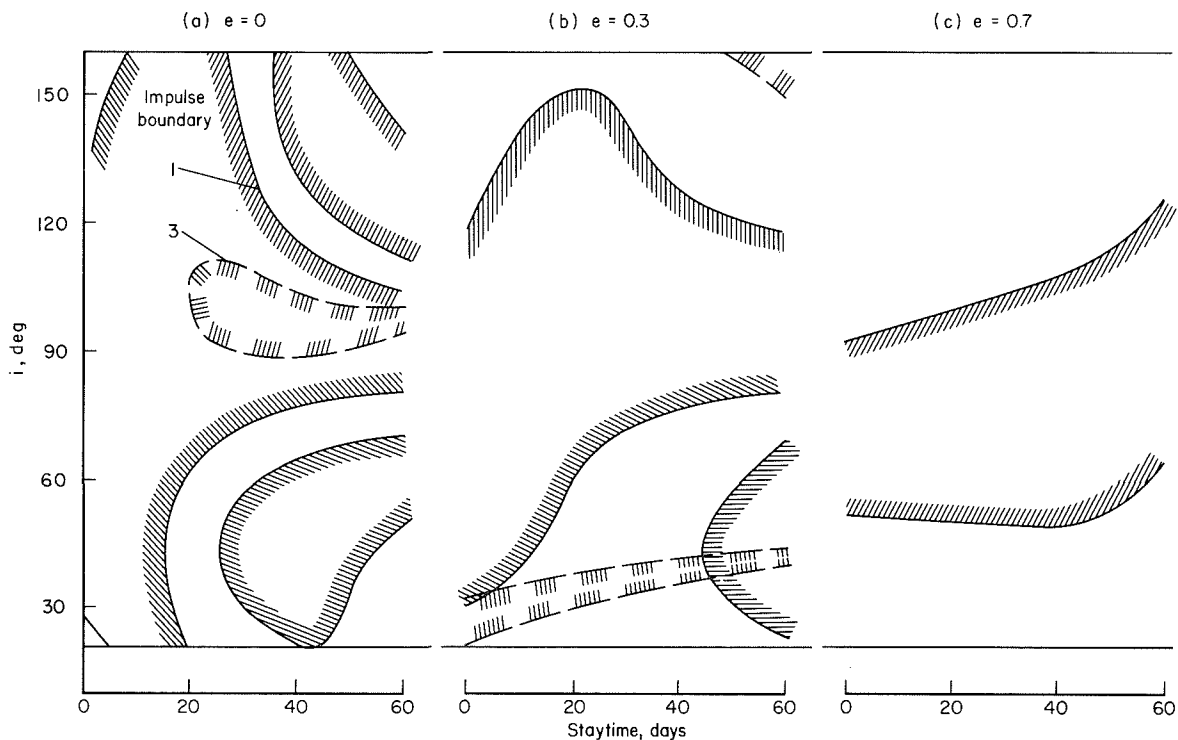


Figure 9.- Effect of eccentricity of launch window 1986; $\Delta V = 7.3$.

The energy level of 7.3 km/sec does not allow a very wide range of staytimes for circular orbits using the single impulse transfer. A ΔV of 8.3 km/sec would allow use of most posigrade orbits (ref. 2). Also, use of the three-impulse transfer technique allows all but a few nearly polar retrograde orbits. Use of medium eccentricity ($e = 0.3$) opens the low-inclination region for single-impulse transfers at this energy level, while three impulses again allow use of all inclinations except an area near 30° inclination. Increasing the orbit eccentricity to 0.7 opens the regions of low

posigrade and almost all retrograde orbits to allow 60-day staytimes. Three-impulse transfers would open the entire region of inclination – staytime shown. As with the 1982 mission, use of the highly elliptical orbit allows lower energies to be considered. Referring to figure 7 reveals that almost the entire region is available for a ΔV of 6.3 km/sec and that all retrograde orbits are available for only 5.3 km/sec where a three-impulse transfer is used. This is a significant reduction from the circular orbit requirements and even from the single-impulse elliptical orbit.

The use of a three-impulse transfer for any orbit eccentricity provides flexibility in the allowable inclination for specific staytimes. This flexibility in choice of inclination has great implications for mission analysis, for it means that the orbit selection and the interplanetary trajectory selection can be decoupled. The orbit therefore can be selected on the basis of scientific goals, experiment requirements, and/or operational requirements without being compromised by interplanetary trajectory considerations.

CONCLUDING REMARKS

Increasing eccentricity of elliptical orbits reduces the total ΔV requirement for a given launch window (staytime). In addition, the use of three impulses to perform the transfer generally requires lower ΔV than does the use of a single impulse. However, orbits can exist (e.g., 1982, $e = 0.7$) for which no gain is shown by the three-impulse maneuver. This situation usually corresponds to a low plane-change requirement. Two specific conclusions can be drawn. First, as a result of the effectiveness of the three-impulse transfer in reducing the ΔV requirement to a nearly constant value regardless of the orbit geometry, the orbit selection can be optimized from other considerations (i.e., science, communication, power, etc.) independent of the interplanetary trajectory considerations. Second, for highly elliptical orbits ($e = 0.7$) a total ΔV (arrival plus departure) at Mars that is 1 km/sec below the minimum coplanar requirement for circular parking orbits provides staytimes of 60 days and usually allows any orbit inclination to be used. This ΔV is effectively 2 km/sec below that required for circular orbits with the same allowable staytime. In addition, whereas the circular orbits require three impulses at departure, for some missions a single impulse can be used to eject from the elliptical orbit.

National Aeronautics and Space Administration
Moffett Field, California 94035, May 14, 1970

APPENDIX A

SINGLE IMPULSE ANALYSIS

Figure 10 indicates the geometry and notation used in the analysis of single impulse escape maneuvers. At the time of departure, the elliptical orbit plane is specified by the longitude of the ascending node Ω (measured from planet Vernal Equinox) and the inclination i . Periapsis of the orbit in this plane is specified by the argument of periapsis ω measured in the orbit plane from the ascending node, and is designated by the unit vector \hat{r}_p . The departure asymptote is specified by two angles: the right ascension ρ and declination δ . The pertinent unit vectors \hat{n} (the normal to the orbit plane) and \hat{V}_∞ are given by

$$\hat{n} = \sin \Omega \sin i \hat{i} - \cos \Omega \sin i \hat{j} + \cos i \hat{k}$$

$$\hat{V}_\infty = \cos \rho \cos \delta \hat{i} + \sin \rho \cos \delta \hat{j} + \sin \delta \hat{k}$$

and the unit vector \hat{r}_p is obtained from

$$\hat{r}_n \times \hat{r}_p = \sin \omega \hat{n}$$

$$\hat{r}_n \cdot \hat{r}_p = \cos \omega$$

where \hat{r}_n is the unit vector at the ascending node and is given by

$$\hat{r}_n = \cos \Omega \hat{i} + \sin \Omega \hat{j}$$

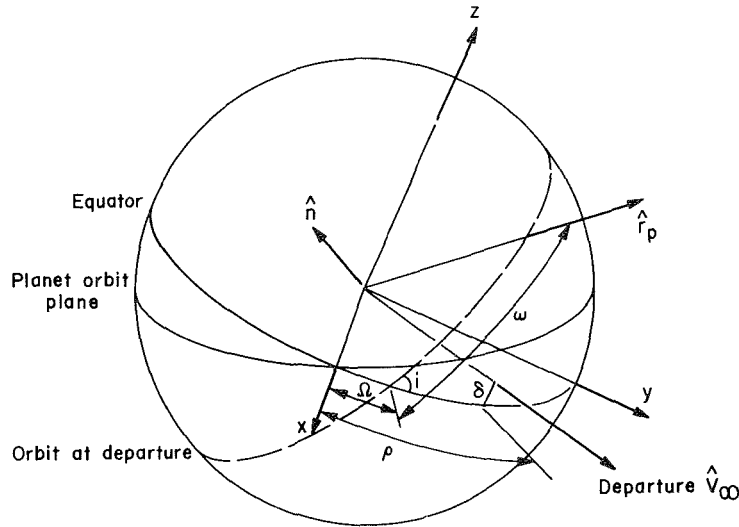


Figure 10.- Orbit geometry.

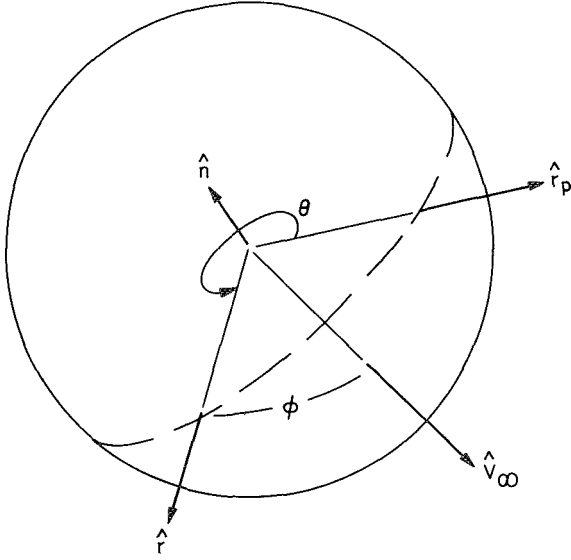


Figure 11.- Ejection point geometry.

Given a true anomaly of departure θ (see fig. 11), the radius of the escape hyperbola is equal to the radius of the ellipse at that point.

$$r = \frac{a_o(1 - e_o^2)}{1 + e_o \cos \theta} = \frac{a_h(1 - e_h^2)}{1 + e_h \cos \theta_h} \quad (A1)$$

where

$$a_h = - \frac{\mu}{V_\infty^2}$$

The angle ϕ between the radius vector, \hat{r} , and the V_∞ vector is given by

$$\cos \phi = \hat{r} \cdot \hat{V}_\infty \quad (A2)$$

where \hat{r} is determined from

$$\hat{r}_p \times \hat{r} = \sin \theta \hat{n}$$

and

$$\hat{r}_p \cdot \hat{r} = \cos \theta$$

Equation (A2) is not explicit, since there are two transfer possibilities for a given point on an ellipse to a given hyperbolic asymptote. One involves a rotation from \hat{r} to \hat{V}_∞ in a positive sense, and the other involves such a rotation in a negative sense. Thus, the angle ϕ determined from equation (A2) has two values, one plus and one minus. The orientation of the two possible departure hyperbolas is shown in figures 12(a) and (b).

The true anomaly on the hyperbola for departure maneuver θ_h is then given by

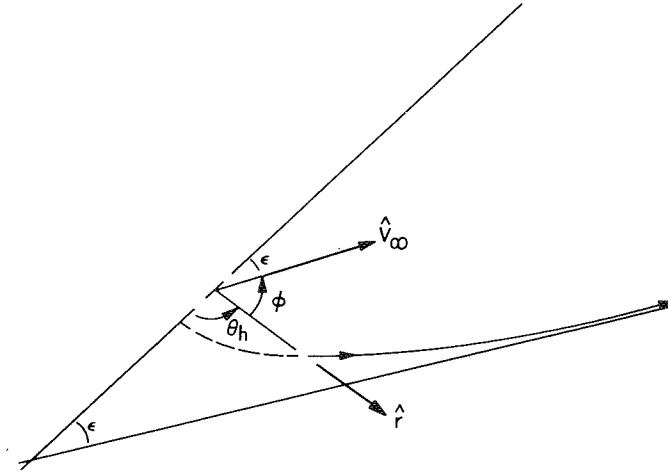
$$\theta_h = \pi - \phi - \epsilon \quad (A3)$$

where

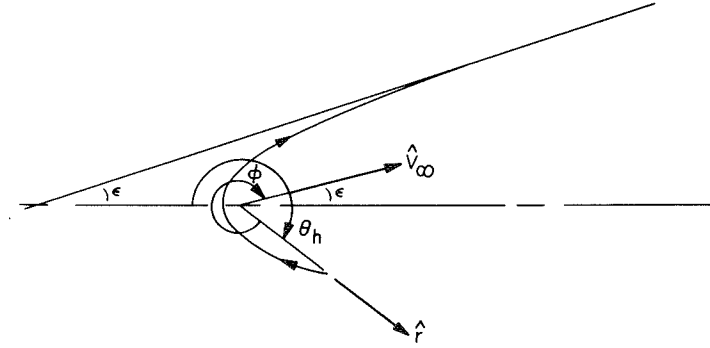
$$\epsilon = \cos^{-1} 1/e_h$$

Noting from equation (A3) that

$$\begin{aligned} \cos \theta_h &= -\cos(\phi + \epsilon) \\ &= -\cos \phi \cos \epsilon + \sin \phi \sin \epsilon \\ &= -\frac{\cos \phi}{e_h} + \frac{\sqrt{1 - e_h^2} \sin \phi}{e_h} \end{aligned}$$



(a) Positive rotation.



(b) Negative rotation.

Figure 12.- Orientation of departure hyperbola.

and substituting into equation (A1) yields

$$r = \frac{a_h (1 - e_h^2)}{1 - \cos \phi + \sqrt{1 - e_h^2} \sin \phi}$$

This equation can be solved for the escape hyperbola eccentricity e_h by substituting $\zeta = \sqrt{e_h^2 - 1}$ and solving the resultant quadratic equation for ζ .

$$\zeta = \sqrt{e_h^2 - 1} = \frac{-r \sin \phi \pm \sqrt{r^2 \sin^2 \phi - 4a_h (1 - \cos \phi)}}{2a_h}$$

The positive radical is not a valid solution since the semimajor axis for a hyperbola is negative and ζ is by definition positive. Therefore,

$$e_h = \left[1 - \frac{r \sin \phi}{2a_h} - \frac{\sqrt{r^2 \sin^2 \phi - 4a_h(1 - \cos \phi)}}{2a_h} \right]^{1/2}$$

The velocity increment vector direction and magnitude to change from the parking elliptical orbit to the escape hyperbola can now be determined through vector analysis as follows. The direction cosines of the unit velocity vector on the ellipse at the point of departure θ are determined by

$$\hat{r} \times \hat{V}_O = \sin \left(\frac{\pi}{2} - \gamma_O \right) \hat{n}$$

and

$$\hat{r} \cdot \hat{V}_O = \cos \left(\frac{\pi}{2} - \gamma_O \right)$$

where the flight path angle γ_O is given by

$$\tan \gamma_O = \frac{e_O \sin \theta}{1 + e_O \cos \theta}$$

Similarly, the direction cosines of the desired unit velocity vector on the escape hyperbola can be determined after the true anomaly on the departure hyperbola is determined from equation (A3) and the unit vector normal to the departure transfer plane is determined from

$$\hat{n}_h = \frac{\hat{r} \times \hat{V}_\infty}{\sin \phi}$$

Then, the unit velocity vector on the hyperbola is given by

$$\hat{r} \times \hat{V}_h = \sin \left(\frac{\pi}{2} - \gamma_h \right) \hat{n}_h$$

and

$$\hat{r} \cdot \hat{V}_h = \cos \left(\frac{\pi}{2} - \gamma_h \right)$$

where the flight path angle γ_h is given by

$$\tan \gamma_h = \frac{e_h \sin \theta_h}{1 + e_h \cos \theta_h}$$

The required velocity increment is then given by

$$\overline{\Delta V} = V_h \hat{V}_h - V_o \hat{V}_o$$

where

$$V_h^2 = \mu \left(\frac{2}{r} - \frac{1}{a_h} \right)$$

and

$$V_o^2 = \mu \left(\frac{2}{r} - \frac{1}{a_o} \right)$$

Since the transfer in a negative rotation sense from a given point on an ellipse to a given hyperbolic asymptote involves passing through periapsis on the departure hyperbola, it is necessary to calculate the periapsis altitude to determine if a positive altitude exists for this transfer. The periapsis altitude is given by

$$H_p = a_h(1 - e_h) - R$$

where R is the radius of the planet.

Finally the optimum departure position on the ellipse is determined by numerical search by stepping true anomaly around the parking ellipse.

APPENDIX B

TWO-IMPULSE ANALYSIS

Figure 10 indicates the geometry and notation used in the analysis of the restricted two-impulse escape maneuver. The description of the geometry at departure is the same as the single-impulse analysis contained in appendix A. The restricted two-impulse maneuver studied here involves an impulse at apoapsis to rotate the parking ellipse coplanar with the departure asymptote followed by a tangential impulse to transfer in that plane from the parking ellipse to the hyperbolic asymptote.

The departure point on the ellipse as shown in figure 13 is designated by the true anomaly θ_i and also by the true anomaly on the escape hyperbola θ_h . The key independent parameter is the angle between the periapsis unit vector \hat{r}_p and the departure asymptote unit vector \hat{V}_∞ , and is designated as P . It is convenient to invert the escape problem and the roles of dependent and independent parameters by specifying θ_i and then determine the resulting angle P .

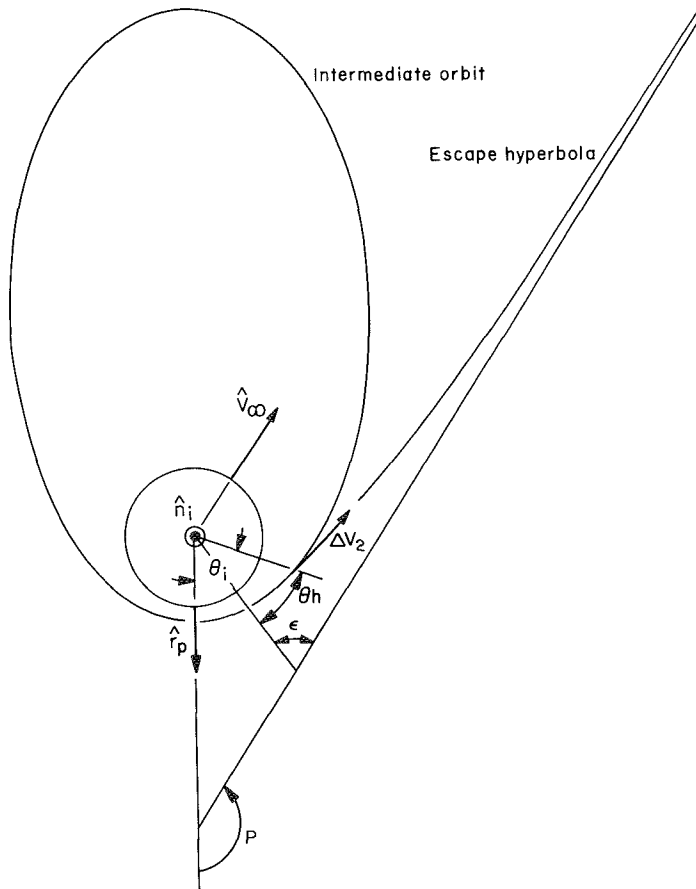


Figure 13.- Escape geometry.

Applying the conditions of tangency between the escape hyperbola and the intermediate ellipse at the point where ΔV is applied and then solving for the unknown eccentricity of the hyperbola yields:

$$e_h = \left[1 - \left(\frac{r}{a_h} \right) \left(\frac{2 - r/a_h}{1 + \tan^2 \gamma} \right) \right]^{1/2}$$

where

$$r = \frac{r_p (1 + e_i)}{1 + e_i \cos \theta_i}$$

$$a_h = - \frac{\mu}{V_\infty^2}$$

and

$$\tan \gamma = \frac{e_i \sin \theta_i}{1 + e_i \cos \theta_i}$$

The true anomaly on the escape hyperbola is then given by

$$\sin \theta_h = \frac{1 - e_h^2}{e_h} \frac{\tan \gamma}{r/a_h}$$

$$\cos \theta_h = \frac{1}{e_h} \left[\left(\frac{1 - e_h^2}{r/a_h} \right) - 1 \right]$$

Referring to figure 13, the asymptote half angle is determined by

$$\epsilon = \cos^{-1} \frac{1}{e_h}$$

and the angle P is finally determined by

$$P = \pi - \epsilon + \theta_i - \theta_h$$

The second velocity increment ΔV_2 is given directly by

$$\Delta V_2 = \left(\mu \frac{2}{r} + V_\infty^2 \right)^{1/2} - \left[\mu \left(\frac{2}{r} - \frac{1 - e_i}{r_p} \right) \right]^{1/2}$$

With reference to figure 10, the unit vector normal to the original orbit plane \hat{n} is given by

$$\hat{n} = \sin \Omega \sin i \hat{i} - \cos \Omega \sin i \hat{j} + \cos i \hat{k}$$

The unit vector, \hat{r}_p , is then determined by

$$\hat{r}_n \times \hat{r}_p = \sin \omega \hat{n}$$

and

$$\hat{r}_n \cdot \hat{r}_p = \cos \omega$$

where \hat{r}_n is the unit vector at the ascending node and is given by

$$\hat{r}_n = \cos \Omega \hat{i} + \sin \Omega \hat{j}$$

The unit vector in the direction of the departure asymptote is given by

$$\hat{V}_\infty = \cos \delta \cos \rho \hat{i} + \cos \delta \sin \rho \hat{j} + \sin \delta \hat{k}$$

and the angle P is determined from

$$\cos P = \hat{r}_p \cdot \hat{V}_\infty$$

The unit vector normal to the departure orbit plane (see fig. 13) is then given by

$$\hat{n}_i = \frac{\hat{r}_p \times \hat{V}_\infty}{\sin P}$$

and thus the plane change angle required at apoapsis to rotate the original orbit plane coplanar with V_∞ is given by

$$\cos \Delta = \hat{n}_i \cdot \hat{n}$$

The required velocity increment is

$$\Delta V_1 = 2 \left\{ \frac{\mu}{r_p} \left[2 \left(\frac{1 + e_i}{1 - e_i} \right) - (1 - e_i) \right] \right\}^{1/2} \sin \frac{\Delta}{2}$$

The total velocity requirement for the escape maneuver is thus given by

$$\Delta V = \Delta V_1 + \Delta V_2$$

REFERENCES

1. Casal, F. G.; Swenson, B. L.; and Masey, A. C.: Elliptic Capture Orbits for Missions to the Near Planets. Proc. Fifth Space Congress, Cocoa Beach, Florida, March 11-14, 1968.
2. Manning, L. A.; Swenson, B. L.; and Deerwester, J. M.: Analysis of Launch Windows From Circular Orbits for Representative Mars Missions. NASA TM X-1651, 1968.
3. Roy, Archie E.: The Foundations of Astrodynamics. The Macmillan Company, N. Y., 1965, p. 224.
4. Gerbracht, R. J.; and Penzo, P. A.: Optimum Three-Impulse Transfer Between an Elliptic Orbit and a Non-Coplanar Escape Asymptote. AAS Paper 68-084, Sept. 1968.
5. Stafford, W. H.; Harlin, S. H.; and Catalfano, C. R.: Parametric Performance Analysis for Interplanetary Missions Utilizing First-Generation Nuclear Stages. NASA TN D-2160, 1964.
6. Stafford, Walter H.; and Catalfano, Carmen R.: Performance Analysis of Chemical Stages in the 300 to 400 Second Specific Impulse Range for Interplanetary Missions. NASA TN D-3153, 1965.



"The aeronautical and space activities of the United States shall be conducted so as to contribute . . . to the expansion of human knowledge of phenomena in the atmosphere and space. The Administration shall provide for the widest practicable and appropriate dissemination of information concerning its activities and the results thereof."

—NATIONAL AERONAUTICS AND SPACE ACT OF 1958

NASA SCIENTIFIC AND TECHNICAL PUBLICATIONS

TECHNICAL REPORTS: Scientific and technical information considered important, complete, and a lasting contribution to existing knowledge.

TECHNICAL NOTES: Information less broad in scope but nevertheless of importance as a contribution to existing knowledge.

TECHNICAL MEMORANDUMS: Information receiving limited distribution because of preliminary data, security classification, or other reasons.

CONTRACTOR REPORTS: Scientific and technical information generated under a NASA contract or grant and considered an important contribution to existing knowledge.

TECHNICAL TRANSLATIONS: Information published in a foreign language considered to merit NASA distribution in English.

SPECIAL PUBLICATIONS: Information derived from or of value to NASA activities. Publications include conference proceedings, monographs, data compilations, handbooks, sourcebooks, and special bibliographies.

TECHNOLOGY UTILIZATION PUBLICATIONS: Information on technology used by NASA that may be of particular interest in commercial and other non-aerospace applications. Publications include Tech Briefs, Technology Utilization Reports and Notes, and Technology Surveys.

Details on the availability of these publications may be obtained from:

SCIENTIFIC AND TECHNICAL INFORMATION DIVISION
NATIONAL AERONAUTICS AND SPACE ADMINISTRATION
Washington, D.C. 20546